Journal of Spectroscopy and Dynamics J. Spectrosc. Dyn. 2013, 3: 19

Vibrational analysis of hydroxyl group in the pyridine n-oxide/trichloroacetic acid complex using the anharmanic approximation and computations of 1D and 2D potential surfaces

G. A. Pitsevich[a,*], A. E. Malevich[a], V. Sablinskas[b], I. U. Doroshenko[c], V. E. Pogorelov[c], V. Balevicius[b]

[a] Belarusian State University, Minsk, Belarus
[b] Vilnius University, Vilnius, Lithuania
[c] Kiev National Taras Shevchenko University, Kiev, Ukraine

[*]Author for correspondence: G. A. Pitsevich, email: pitsevich@bsu.by
Received 22 Dec 2012; Accepted 21 Jan 2013; Available Online 21 Jan 2013

Abstract

The geometry optimization for the pyridine N-oxide/trichloroacetic acid complex is realized in $B3LYP/cc-pVTZ$ approximation. Computations of IR absorption spectra for the optimized configuration are performed in harmonic and anharmonic approximations. It is found that taking into account the anharmonicity effects leads to the red shift of the stretching vibration frequency of $O-H$ bond by more than 600 cm^{-1}. At the same time, the red shift of the in-plane and out-of-plane bending vibrations of the hydroxyl group does not exceed 70 cm^{-1}. The 1D potential curves and 2D potential surfaces associated with stretching and bending vibrations of a hydroxyl group are computed. The vibrational frequencies of $O-H$ bonds are derived by numerical solution of Schrödinger equations. The frequencies are compared to those of anharmonic computations for this complex. A combined method including the advantages of both approaches is proposed.

Keywords: H-bond; Anharmonic approximation; 1D and 2D Schrödinger equations

1. Introduction

Recent activities in the hydrogen bond (H-bond) research indicates unabated interest on this type of interactions having a key role in many physical or chemical and biochemical processes, crystal engineering, technologically relevant materials, etc [1-4]. Because of its abundance and importance in the molecular world and beyond there is continual debate on definition of the term "H-bond" in general [5,6]. Quantitave estimations of its strength, subtle influence of media to it, cooperativity and proton/deuteron transfer effects [7-9] are in focus of investigations too. Really boosting interest is observed in short strong H-bonds [10,11]. The detailed understanding of short and very short H-bonds with large-amplitude proton dynamics is challenging task that requires joint efforts of the best available experimental techniques and the most advanced theoretical treatments [12-15]. Pyridine N-oxide (PyO) or its derivatives [16] in the complexes with various acids can be used as very convenient model systems to improve the understanding of the nontrivial physical features of short H-bonding [10,17,18]. Such systems exhibit in many cases very asymmetric and rather flat H-bond potentials, which allow large-amplitude proton motion with the possible proton transfer through such linkages [10,11]. The pyridine N-oxide/trichloroacetic acid ($PyO\cdot TCA$) complex has been chosen for studies in the present work for several reasons. Firstly, high-quality neutron- and X-ray diffraction, as well as some basic vibrational spectroscopy using inelastic neutron scattering [10 and the Refs therein] and infrared absorption [18] data are available for this system. Secondly, the results of several DFT computational models covering range from the isolated gas phase clusters to periodic boundary conditions, viz. CPMD, CRYSTAL and VASP. Thirdly, using B3LYP and PBE0 functional with the polarizable continuum model (PCM) to model bulk effects of the acetonitrile solvent have been published [10,18,19]. However, in all these cases the vibrational frequencies were calculated in harmonic approximation.

The literature sources on computations of the IR spectra even for the simplest complexes with a hydrogen bond using the anharmonic approximation are just a few available. Analyzing the spectral region of $O-H$ stretching vibrations in the complexes [20] $CH_3NO_2^-\cdot(H_2O)$ and $CH_3CO_2^-\cdot(H_2O)$, the authors have restricted themselves to computations of the cubic force constants and demonstrated a good correlation with the experiment. Such good correlation can be explained by the fact that a hydrogen bond in such a system is weak - the absorption band of $O-H$ stretch in these complexes in gaseous samples [21] is located close to 3400 cm^{-1}. Based on analysis of the in- and out-of-plane hydroxyl group bending vibrations in monomeric and dimeric benzoic acid, the authors [22] have indicated that the anharmonic approximation fails in computations of the frequencies for out-of-plane vibrations. They necessitate the computation of the 1D and 2D potential surfaces, associated with these vibration, by means of numerical solution of Schrödinger equation. Similar 3D computations have been performed for analysis of the $O-H$ bond stretching vibrations in the cyclic dimer of formic acid [23]. The potential surface exhibits two minima separated by the potential barrier. Presence of the barrier is reason for various peculiarities of IR and Raman spectra of such complexes. It is to be noted that detailed comparison of computational results in harmonic and anharmonic approximations does not exist till now. The situation is even more complicated in the case of complexes, where the intermolecular hydrogen bonds are short or very short. As it is noted in [10], INS and IR spectra of the complex under study and DFT computations of the vibrational spectra

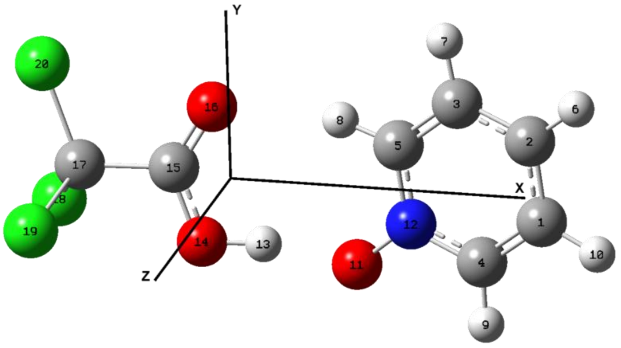

Figure 1. Pyridine and trichloroacetic acid complex with indication of atomic numbers and Cartesian axes directions.

in the harmonic approximation provide no conclusive information concerning the stretching vibration of a hydroxyl group. According to [24], shortening of the distance between X atoms in the chain $X-H\cdots X$ is accompanied by shift of a hydrogen atom towards the half distance between X atoms. From the results of $MP2/cc-pVDZ$ computations [24], just this symmetric position is occupied by a proton in complexes of the type $(H_2O)_2H^+$, $(Me_2O)_2H^+$ and $(Et_2O)_2H^+$, where the distance $O\cdots O$ is less than 2.4Å. Owing to a simplified form of the potential, the harmonic approximation gives quite adequate predictions for frequencies of stretching vibrations of the hydroxyl group [24]. It is expected that the most serious difficulties in vibrational analysis of a hydroxyl group may arise in complexes with medium and short lengths of the hydrogen bridge $X-H\cdots X$. The complex studied is compound of such a type. It is important to compare the computational results for the hydroxyl group vibrational frequencies in harmonic and anharmonic approximations with the data obtained using 1D, 2D computations of the potential surfaces as well as to combine the advantages of both methods.

2. Computational methods

Computations of the spectral and structural characteristics of TCA and $PyO\cdot TCA$ were performed using the package GAUSSIAN 09 [25] in the approximation $\mathrm{B3LYP/cc-pVTZ}$. B3LYP is one of the approaches in a density functional theory (DFT) designed to include the exchange and electron correlation effects. This approach is a well known and widely used as a hybrid method combining five functionals: Three of them take into account the exchange effects (Becke + Slater + HF) and two of them (B3LYP + VWN5) take into account electron correlation [26-28]. A series of the correlation-coordinated and valence-split sets of the Dunning basis functions [29] having the general form $\mathrm{cc-pVXZ}$, where $\mathrm{X=D,T,Q,5,6}$ and so on, consistently approach a complete set of basis functions. As shown by our previous studies, computations in the approximations $\mathrm{B3LYP/cc-pVDZ}$ and $\mathrm{B3LYP/cc-pVTZ}$ reproduce well frequencies of the harmonic vibrations and the shape of the potential-surfaces for some organic molecules [30,31]. In the process of optimization of the geometry for these compounds, the fact that minima on the potential surface were reached has been supported by the absence of imaginary frequencies in vibrational spectra. IR spectra of these compounds were computed in the harmonic and anharmonic approximations. In case of the latter the frequency shifts of the fundamental vibrations due to Fermi and Darling-Dennison resonances were included as well. The potential energy distribution (PED) of the normal modes were calculated using standard options of GAUSSIAN 09 package [25]. The equilibrium configuration of the complex, atomic numbers, and positions of the Cartesian axes are shown in Figure 1.

As seen in Figure 1, X axis is practically parallel to the hydroxyl bond lying in the plane XOY. It is clear that motion of the hydrogen atom along the axis X may be associated with the stretching vibration, whereas its motion along the axis Y may be associated with the in-plane and along the axis Z -- out-of-plane bending vibrations of the hydroxyl group. During the computations it was assumed that motion of a hydrogen atom is independent of other atoms in the molecule within the potential field formed between two oxygen atoms. We have computed the complex energies at more than 300 points by positioning the atom $\mathrm{H_{13}}$ at the certain nodes of 1D and 2D meshes, without geometrical optimization of the complex for the remaining geometrical parameters.

3. Results of harmonic and anharmonic computations of IR spectra for PyO.TCA complex

As evidenced by the computations, the eight membered cycle of the complex is not flat. The dihedral angle between the plane of a pyridine ring and the plane, where the atoms $\mathrm{H_{13}}$, $\mathrm{O_{14}}$, $\mathrm{C_{15}}$, $\mathrm{O_{16}}$, and $\mathrm{C_{17}}$ are located is $158.3°$. The distance between the oxygen atoms is short - 2.578 Å. Proton is far from the middle of the distance between oxygen atoms (bond length of a hydroxyl group is 1.016 Å and length of the hydrogen bond - 1.573 Å). The computed angle of $\mathrm{O\cdots H-O}$ comes to 168.9^0. In order to find in the $\mathrm{B3LYP/cc-pVTZ}$ approximation, the value for the red shift of the stretching vibration of the hydroxyl group when the complex is formed, geometrical optimization was performed and the fundamental vibration frequencies were computed in the harmonic and anharmonic approximations for a molecule of trichloroacetic acid (see Figure 1, atoms 13 - 20). Values of the vibrational frequencies of a hydroxyl bond for TCA molecule and $\mathrm{PyO\cdot TCA}$ complex are listed in Table 1.

According to the computations, more than 99% of the PED of the sixth mode with the frequency $2822.4\ \mathrm{cm^{-1}}$ is related to the hydroxyl group stretching vibration. In this way in the harmonic approximation the vibration is highly localized, i.e. it is not mixed with the other normal modes. Bending vibrations of the hydroxyl group in the complex take part in several normal modes. The principal contributions into PED of in-plane and out-of-plane bending vibrations of $\mathrm{O-H}$ group are associated with the normal vibrations at the frequencies 1488.5 and $1003.3\ \mathrm{cm^{-1}}$ which are as large as 70% and 65%, respectively. As seen from Table 1, when the complex is formed, ν_{OH}, is subjected to a significant bathochromic shift ($1346\ \mathrm{cm^{-1}}$), being indicative of the hydrogen bond strength. Both in the acid monomer and in the complex this vibration is anharmonic but a degree of anharmonicity in the complex is considerably higher (the ratio $\frac{|\Delta\nu|}{\nu}$ in trichloroacetic acid is 5.3% for the acid while it is 21.9% for the complex). Analysis of the anharmonic constants $\chi_{i,j}$ allows us to conclude that the major factor determining

Table 1. Frequencies of harmonic and fundamental vibrations and of the first overtones for a hydroxyl group in TCA molecule and PyO.TCA complex.

Vibration modes	**TCA**			**PyO.TCA**			
	Harmonic frequency	**Fundamental frequency**	**Overtone frequency**	**Number of fundamental vibration**[a]	**Harmonic frequency**	**Fundamental frequency**	**Overtone frequency**
	(cm^{-1})	(cm^{-1})	(cm^{-1})		(cm^{-1})	(cm^{-1})	(cm^{-1})
ν_{OH}	3748.3	3548.6	6922.5	6	2822.4	2203.6	3783.0
δ_{OH}^{ip}	1361.4	1345.6	2240.1	12	1488.5	1417.6	2833.0
δ_{OH}^{oop}	549.3	484.1	927.4	23	1003.3	959.4	1839.0

[a] Number of fundamental vibration in complex, involving hydroxyl group

considerably lower frequencies of the fundamental stretching vibration of O − H bond as compared to the harmonic value is anharmonicity of this vibration per se. Indeed, the value $\chi_{6,6} = -337.5\ \mathrm{cm}^{-1}$ is much higher than all other anharmonicity constants. Besides, there is an anharmonic force interaction of the modes associated with stretching and bending vibrations of a hydroxyl group. But in the case of interaction with the in-plane bending vibration the frequencies of both vibrations are lowered ($\chi_{6,12} = -82.3\ \mathrm{cm}^{-1}$), while the interaction with an out-of-plane bending vibration leads to an increase in the frequencies of both vibrations ($\chi_{6,23} = 176.8\ \mathrm{cm}^{-1}$). So, a partial compensation for the interaction effects on the frequency of the O − H stretching vibration takes place. One should remember that non-diagonal anharmonicity constants have the weighting factor 0.25 relative to the diagonal constants during computations of frequencies for fundamental vibrations [32]:

$$\nu_i^{\mathrm{fund}} = \omega_{0,i} + 2\chi_{i,i} + \frac{1}{2}\sum_{j\neq i}^{N} \chi_{i,j}\,, \qquad (1)$$

where $\omega_{0,i}$ - harmonic frequency of the i-th fundamental vibration. Anharmonicity of the out-of-plane bending vibrations associated with acid is greater than that of the complex: the value of $\frac{|\Delta\nu|}{\nu}$ for the acid comes to 11.9% and for the complex - to 4.4%. The latter is due to the fact, that the formation of the hydrogen bond results in a higher barrier of the internal rotation of a hydroxyl group about $\mathrm{C-O}$ bond. As $\chi_{12,12} = -6.0\ \mathrm{cm}^{-1}$ and $\chi_{23,23} = -39.7\ \mathrm{cm}^{-1}$, anharmonicity of the potential curve along the axis Y should be lower than that along the axis Z. The anharmonic interaction of the modes of bending vibrations is low ($\chi_{12,23} = -4.5\ \mathrm{cm}^{-1}$). Thus, a frequency decrease of the in-plane bending vibration is primarily caused by the anharmonic interaction with the stretching vibration of a hydroxyl group. At the same time, red shift of the out-of-plane bending vibration could be greater, but for the force anharmonic interaction of this mode with ν_{OH}.

4. 1D potential curves

The motion of the hydrogen atom between the oxygen atoms may be described in different ways. Firstly, one can use the normal modes as coordinates [22]. In this case the motion of the H atom may be accompanied by motions of other atoms and entire fragments of the complex. The reduced mass and potential energy are calculated at the mesh for various mode amplitudes. Secondly [33], the complex geometry may be optimized at every displacement step of H along one of the axes X, Y or Z. In this case the moving proton follows the path of minimal energy and its motion may also be accompanied by the motion of other atoms in the complex. Thirdly [34,35], it is supposed that the motion of the hydroxyl hydrogen atom does not contribute to other fundamental vibrations and hence the potential energy of the complex at the mesh of the displaced positions of H may be computed without the geometry optimization. When used for different molecular complexes, all these three approaches exhibit good agreement with the experiment. Because of this, selection must be performed with due regard for the features of a problem at hand. As noted in [33], the second approach may be associated with a problem of inertia of the molecular fragments. As a consequence, this approach is more appropriate for light carboxylic acid studied in [33] than for the complex under study in this work. Since the normal mode for the stretching vibration of a hydroxyl group is by 99% attributed to changes in the length of $\mathrm{O-H}$ bond, the first and second approaches in essence become similar. Considering that the modes of bending vibrations of a hydroxyl group are mainly attributed to changes in the corresponding valence and dihedral angles, the authors have chosen the third approach to describe the motion of the hydroxyl group in the studied complex. As already mentioned, the stretching vibration of the hydroxyl group was associated with the motion of a hydrogen atom along the axis X.

The energies were computed in the approximation $\mathrm{B3LYP/cc-pVTZ}$ for the displacements by 0.5 Å in the direction of the valence-bonded oxygen and by 1.1 Å in the direction of the acceptor oxygen. In between the energy was computed at the points having a spacing of 0.1 Å. Along the axes Y and Z the amplitude of displacements was ±0.7Å, again with the spacing 0.1 Å. Positions of all the atoms, excluding the hydroxyl hydrogen atom, were consistent with the optimized configuration. Figure 2 shows the potential energy of the complex as a function of the hydrogen atom displacement along the axis X. As seen from Figure 2, there is single minimum at the equilibrium position. The curve is highly asymmetric, but asymmetry of the potential being not so significant at the energies within the interval from 0 to $3800\ \mathrm{cm}^{-1}$. Within the energy interval from 3800 to $6000\ \mathrm{cm}^{-1}$ a slope of the cure at the left is drastically

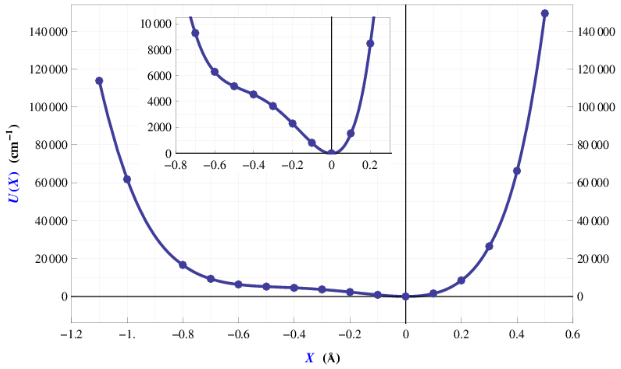

Figure 2. Potential energy of the complex as a function of the hydrogen atom displacement along *X* axis.

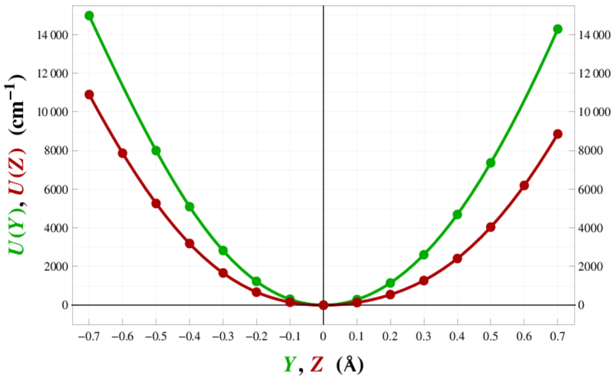

Figure 3. Potential energy of the complex as a function of the hydrogen atom displacement along *Y*, Z axis.

diminished, that in this case should lead to convergence of the stationary energy levels. Then a slope of the function at the left is raised again and hence we could expect an increase in the spacing between the energy levels above $6000\ \mathrm{cm}^{-1}$. The relationship between the potential energy of the complex and the hydrogen atom displacement along the axes Y and Z is shown in Figure 3.

It can be seen in Figure 3 that the potential functions are much more symmetric having nearly parabolic shape. The later is especially true for the U(Y) function. Based on the energy values computed at the nodes, the potential function was approximated using *Mathematica* package [36] by the fourteenth-degree (X coordinate) and eighth-degree (Y and Z coordinates) polynomials expressed as $U'(x)=\sum_{k=2}^{m}u_k x^k$. A search for the stationary energy states in the case of 1D potential wells was realized in two ways. The first approach is described in [37] and used for the 1D case only. The Schödinger equation takes the form:

$$-R\frac{d^2\Psi(x)}{dx^2}+U'(x)\Psi(x)=E'(x)\Psi(x). \qquad (2)$$

Here and hereinafter x is assumed as any of the dimensionless variables x, y, z defined as $x=\frac{X}{l_0};\ l_0=1\text{Å}$. And the constant R is given as $R=\frac{\hbar^2}{2m_H l_0^2}=16.735\ \mathrm{cm}^{-1}$. Using (2), we can express the second derivative of the wave function as follows:

$$\frac{d^2\Psi(x)}{dx^2}=\left(U(x)-E\right)\Psi(x), \qquad (3)$$

where $U(x)=U'(x)/R$ and the derived polynomial presentation of the potential function is used as $U'(x)$. The variability domain of x ($L=x_{end}-x_{start}$) was divided into equal segments Δx to meet $L/\Delta x=N$, where $N\in\mathbb{N}$ and $N\gg 1$. Specifying the first-segment-beginning coordinate x_0, for the coordinate of the i-th segment ending we have $x_i=x_0+i\Delta x$, where i takes the numerical values from 1 to N. Then the initial values of $\Psi(x_0)$ and $\Psi'(x_0)$ are given. The value of $\Psi''(x_0)$ is computed from (3). Next, the values of the wave function and its first derivative are computed at the end of the first segment using the following formulas:

$$\Psi'(x_1)=\Psi'(x_0)+\Psi''(x_0)\Delta x, \qquad (4)$$

$$\Psi(x_1)=\Psi(x_0)+\Psi'(x_0)\Delta x. \qquad (5)$$

The process is repeated until x_i becomes greater than x_{end}. To capture and to find a position of the stationary energy level, we use the fact that the wave function is divergent in different directions beyond the boundary of a potential well for the energies over and below the stationary level energy. Zeros checking embedded into the algorithm for the wave function allows one to exclude the omission of some stationary state. Written in the Fortran, this program was tested for the harmonic oscillator and the oscillator with Morse and Slater potentials having an analytical solution. The computed energies of stationary states and the frequencies of some transitions for three potential wells are listed in Table 2.

Note that the level arrangement at the potential well associated with the motion along the axis X (see Table 2) is in a complete agreement with the foregoing quantitative considerations based on the potential curve form.

Now we proceed to the second approach to solution of the type (2) Schrödinger equation. The previously derived polynomial representation of the potential energy function was used for the Fourier-series expansion of the following form:

$$U(x)=\sum_{k=-a}^{a}u_k\exp\left(ik\frac{2\pi}{L}x\right);\quad a,b\in\mathbb{N}, \qquad (6)$$

where L is still the variability domain of x coordinate but the value of L is different from that used in the first approach. Here the initial and the final value of x was selected proceeding from the requirement for approximate equality of the energies at these points and for the energy value sufficient to determine reliably the energies associated with several most deeply-lying stationary states. From Figures 2 and 3 the initial and the final values of x were determined as −1.0 and 0.4; −0.7 and 0.7; −0.6 and 0.6 Å for X, Y, and Z. The wave function is derived as:

$$\Psi(x)=\sum_{n=-\infty}^{\infty}b_n\exp\left(in\frac{2\pi}{L}x\right). \qquad (7)$$

Table 2. Computed energies of the stationary states and frequencies for some transitions caused by the hydroxyl group vibrations (first approach).

The energies of the stationary states				**Frequencies of transitions**			
Level number	ν_{OH} (cm^{-1})	δ_{OH}^{ip} (cm^{-1})	δ_{OH}^{oop} (cm^{-1})	**Transitions** $n'' \Rightarrow n'$	ν_{OH} (cm^{-1})	δ_{OH}^{ip} (cm^{-1})	δ_{OH}^{oop} (cm^{-1})
$n = 0$	1306.6	705.7	504.1	$0 \Rightarrow 1$	2269.3	1415.9	1034.4
$n = 1$	3575.9	2121.6	1538.5	$1 \Rightarrow 2$	1697.8	1428.3	1082.9
$n = 2$	5273.7	3549.9	2621.4	$2 \Rightarrow 3$	1432.4	1436.3	1119.7
$n = 3$	6706.1	4986.2	3741.1	$3 \Rightarrow 4$	1606.1	1439.7	1146.0
$n = 4$	8313.1	6425.9	4887.1	$4 \Rightarrow 5$	1794.5	--	--
$n = 5$	10107.7	--	--	$5 \Rightarrow 6$	1955.7	--	--
$n = 6$	12063.4	--	--	$0 \Rightarrow 2$	3967.1	2844.2	2117.3

Substituting (6) and (7) into (2), we can form the nominally infinite Hamiltonian matrix that must be truncated for some finite value of n in (7), sufficient for stabilization of some smallest eigenvalues. This solution is given in greater detail in [38]. Table 3 presents the stationary level energies and the frequencies of some transitions for three potential wells computed by this method using the *Mathematica* package [36]. Based on comparison of the data in Tables 2 and 3, we can state that as a whole there is a good agreement between the computational results of two approaches. This is especially true for the fundamental vibrational frequencies. The best correlation of the energy level positions is observed for the most symmetric potential well associated with the motion of a hydrogen atom along the axis Y. For two remaining potential wells we can observe the tendency for the increasing divergence in the computational results in two approximations with the growing energy of the levels. This may be attributed to a significant asymmetry of these potential wells. Consequently, representation of the potential energy as a Fourier series becomes complicated, Gibbs beats occur to increase the computational errors. As a whole, the first approach is preferable as an asymmetric aperiodic potential may be better approximated both at the specified points and between the points with the use of power polynomials. Comparing the results in Tables 1-3, as a whole, we can point to a satisfactory agreement between the fundamental vibration frequencies of a hydroxyl group and their overtones, computed in the anharmonic approximation, and the frequencies for the corresponding vibrations, computed using the two numerical methods.

5. 2D potential surfaces

The potential energy values in the plane xOy, where xOy is understood as any of the planes XOY, XOZ or YOZ, were computed at the nodes of a 2D mesh with a spacing of 0.1 Å for each of the coordinates. The computational area was represented by a rectangle the boundaries of which were determined by the requirement to embrace the contour with a specified energy sufficient for finding the positions of some deepest-lying stationary levels. For every plane, the energy was computed at more than 100 points. Further computations were performed using the *Mathematica* package [36]. First, the potential surface was approximated by a power polynomial of the form:

$$U(x,y) = \sum_{k,l=1}^{m,n} u_{k,l} x^k y^l, \tag{8}$$

where m and n were derived proceeding from the requirement for minimization of the root-mean-square discrepancies in the energy at the mesh nodes, not exceeding a maximum degree of the polynomials found in the process of 1D computations for every coordinate. With the use of the analytical expression thus obtained for the 2D potential energy (8), the mesh at the initial rectangles was congested. Using (8), we have computed the energy at the points between the nodes so as to provide for each of the axes a spacing less than 0.1 Å. These points, along with the initial ones, were used to approximate the potential surface with the help of 2D Fourier series of the following form:

$$U(x,y) = \sum_{k,l=-a,-b}^{a,b} u_{k,l} \exp\left(i2\pi\left(\frac{kx}{L_x} + \frac{ly}{L_y}\right)\right); \quad a,b \in \mathbb{N}, \tag{9}$$

where L_x and L_y - lengths of the rectangle sides along the axis x and y, respectively. The form of the computed 2D potential surfaces is demonstrated in Figure 4.

As seen in Figure 4, complexity of the potential surfaces is growing as follows: YOZ → XOY → XOZ. The wave function takes the form:

$$\Psi(x,y) = \sum_{n,m=-\infty}^{\infty} b_{n,m} \exp\left(i2\pi\left(\frac{nx}{L_x} + \frac{my}{L_y}\right)\right). \tag{10}$$

A Schrödinger equation is of the following form:

$$-R\frac{\partial^2\Psi(x,y)}{\partial x^2} - R\frac{\partial^2\Psi(x,y)}{\partial y^2} + U(x,y)\Psi(x,y) = E\Psi(x,y). \tag{11}$$

Substituting (9) and (10) into (11), we can construct a Hamiltonian matrix and then use the solution presented in [38]. The resultant frequencies for fundamental vibrations of a hydroxyl group are listed in Table 4.

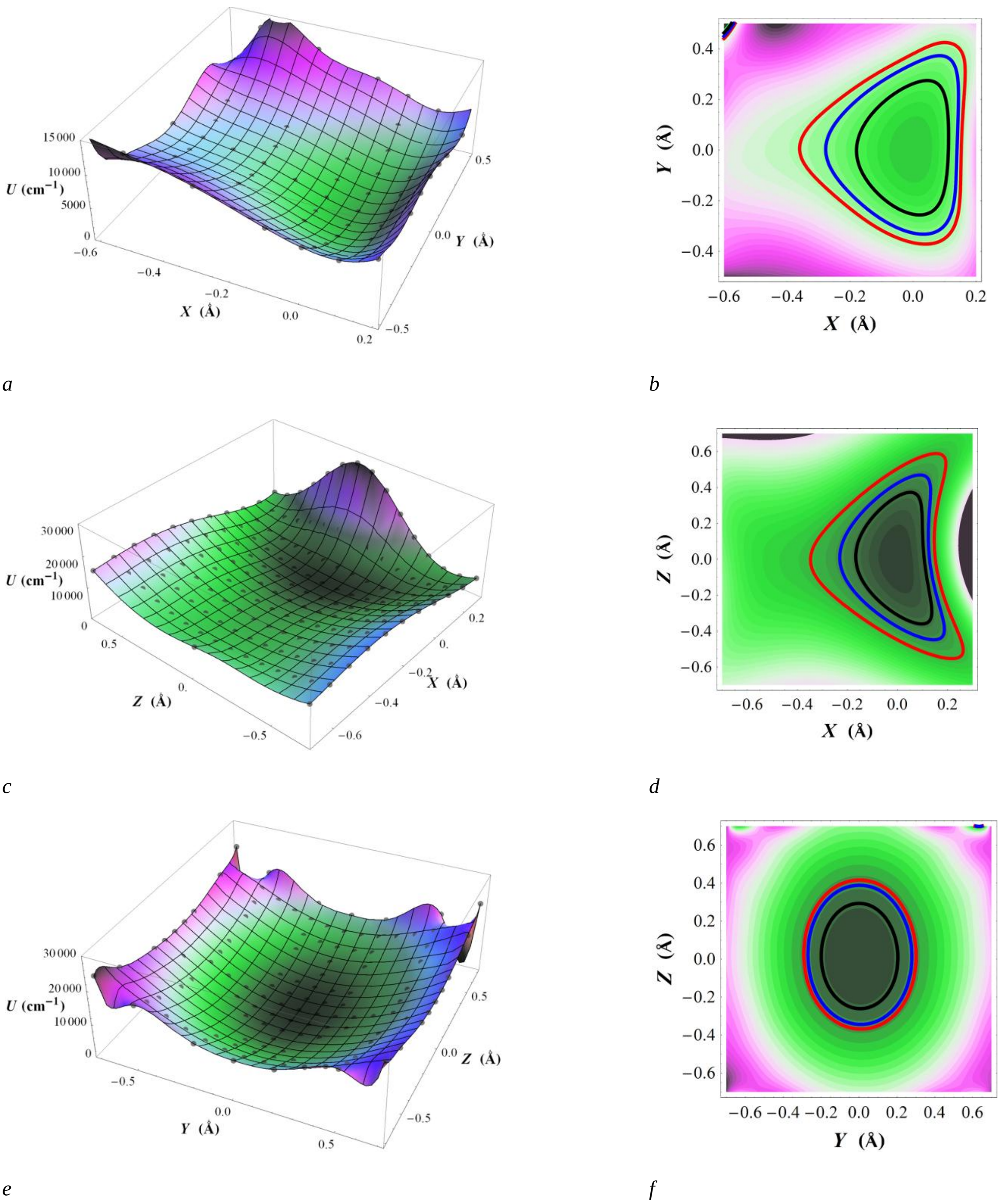

a *b* *c* *d* *e* *f*

Figure 4. 3D and 2D potential surfaces associated with the motion of a hydroxyl hydrogen atom within the planes *XOY* (a,b), *XOZ* (c,d), and *YOZ* (e,f).

Based on analysis of the data in Tables 2-4, we can conclude that, despite the absence of the kinematic interaction, there is a force interaction for the two-dimensional motion of a hydroxyl hydrogen atom. In Figure 4(b,d,f) the profile for the constant energy of zero vibration is black and the profiles for fundamental vibrations with lower and higher frequency are blue and red, respectively. Most simple profiles elliptic in form are characteristic for vibrations within the plane YOZ (Figure 4f). The forms of profiles within the planes XOY and XOZ (Figure 4(b,d)) point to a higher vibration amplitude. This is supported by the wave functions associated with the $O-H$ group fundamental vibrations (Figure 5). As seen from Figure 5(a,b), two maxima of the square wave function for the $O-H$ group bending vibrations are positioned along the axes Y and Z, symmetrically about the origin of coordinates. In the case of the hydroxyl group stretching vibration, two maxima of the Ψ^2 are non-equivalent. Coordinates of the global maximum Ψ^2 within the planes XOY and XOZ are as follows: $(-0.2$ Å; 0.0 Å). There is a non-zero probability that a proton may be found for the values of X up to -0.4 Å. Coordinates of the second maximum within these planes are (0.1 Å; 0.0 Å), and the probability of finding a proton for $X \geq 0.2$ Å is zero. Besides, in the case of ν_{OH} there is a non-zero probability

Table 3. Computed stationary state energies and frequencies of some transitions due to the hydroxyl group vibrations (second approach).

The energies of the stationary states				Frequencies of transitions			
Level number	ν_{OH} (cm^{-1})	δ_{OH}^{ip} (cm^{-1})	δ_{OH}^{oop} (cm^{-1})	Transitions $n'' \Rightarrow n'$	ν_{OH} (cm^{-1})	δ_{OH}^{ip} (cm^{-1})	δ_{OH}^{oop} (cm^{-1})
$n = 0$	1287.3	705.5	504.7	$0 \Rightarrow 1$	2262.7	1416.4	1040.0
$n = 1$	3550.0	2121.9	1544.7	$1 \Rightarrow 2$	1654.4	1428.2	1101.4
$n = 2$	5204.4	3550.1	2646.0	$2 \Rightarrow 3$	1363.3	1437.3	1171.3
$n = 3$	6567.6	4987.4	3817.4	$3 \Rightarrow 4$	1566.6	1442.4	1263.8
$n = 4$	8134.2	6429.8	5081.2	$4 \Rightarrow 5$	1760.7	1447.5	--
$n = 5$	9894.9	7877.4	--	$5 \Rightarrow 6$	1923.5	--	--
$n = 6$	11818.4	--	--	$0 \Rightarrow 2$	3917.0	2844.6	2141.4

Table 4. The vibration frequencies of a hydroxyl group obtained using 2D approach.

Vibration modes	Fundamental frequency (cm^{-1})			Overtone frequency (cm^{-1})			Combination frequency (cm^{-1})		
	XOY	XOZ	YOZ	XOY	XOZ	YOZ	XOY	XOZ	YOZ
ν_{OH}	2244.0	2337.9		3903.1	4425.6		3606.3	2718.5	
δ_{OH}^{ip}	1380.7		1426.0	2725.6		2835.3	3606.3		2486.5
δ_{OH}^{oop}		962.0	1045.2		1852.6	2037.7		2718.5	2486.5

of finding a proton for significant nonzero values of Y and especially of Z (Figure 5(c,d)).

6. Results and Discussion

Earlier we have compared the frequencies obtained for fundamental vibrations of a hydroxyl group in the anharmonic approximation to the results of 1D computations, though such a direct comparison is somewhat incorrect. It seems better to compare the 1D computational results with the value predicted by the anharmonic approximation for a single coordinate:

$$\nu_i^{\mathrm{anharm}} = \omega_{0,i} + 2\chi_{i,i} \,. \qquad (12)$$

Considering that $\chi_{6,6} = -337.5\ \mathrm{cm}^{-1}$, $\chi_{12,12} = -6.0\ \mathrm{cm}^{-1}$, $\chi_{23,23} = -39.7\ \mathrm{cm}^{-1}$, and $\omega_{0,6} = 2822.4\ \mathrm{cm}^{-1}$, $\omega_{0,12} = 1488.5\ \mathrm{cm}^{-1}$, $\omega_{0,23} = 1003.3\ \mathrm{cm}^{-1}$, with the use of (12) we derive the following frequencies: $\nu_6^{\mathrm{anharm}} = 2147.4\ \mathrm{cm}^{-1}$, $\nu_{12}^{\mathrm{anharm}} = 1476.5\ \mathrm{cm}^{-1}$, $\nu_{23}^{\mathrm{anharm}} = 923.9\ \mathrm{cm}^{-1}$. Comparison of the latter three values with the data in Tables 2 and 3 (transition $0 \Rightarrow 1$) reveals that the anharmonic approximation underestimates the frequencies of stretching and out-of-plane bending vibrations of a hydroxyl group and overestimates the frequencies of an in-plane bending vibration. Values of the frequencies ν_{OH} and $\delta_{\mathrm{OH}}^{\mathrm{ip}}$ are decreased on going from 1D X, 1D Y to 2D XOY computations approximately by 25 and 35 cm^{-1}, respectively.

Qualitatively, such a behavior corresponds to the value $\chi_{6,12} = -82.3\ \mathrm{cm}^{-1}$, according to which the anharmonic interaction of these modes should lead to lowering of the vibration frequencies by $41.2\ \mathrm{cm}^{-1}$. As $\chi_{12,23} = -4.5\ \mathrm{cm}^{-1}$, in the anharmonic approximation the interaction of deformation modes is insignificant and should result in the lowered frequencies of both modes - by $2.3\ \mathrm{cm}^{-1}$. From comparison of the results for 1D Y, 1D Z, and 2D YOZ computations it is found that the interaction of these modes is minor but values of the frequencies for both vibrations are increased by about $10\ \mathrm{cm}^{-1}$ rather than decreased. The situation is different for the coordinates X and Z. Since $\chi_{12,23} = 176.8\ \mathrm{cm}^{-1}$, the anharmonic interaction of the modes should lead to the frequencies of both stretching and out-of-plane bending vibrations of $\mathrm{O-H}$ group growing by $88.4\ \mathrm{cm}^{-1}$. However, comparison of 1D X, 1D Z, and 2D XOZ computations points to the fact that ν_{OH} is actually growing by $67.7\ \mathrm{cm}^{-1}$, whereas $\delta_{\mathrm{OH}}^{\mathrm{oop}}$ is decreased by $72.4\ \mathrm{cm}^{-1}$. As seen from (1), the interaction of two normal modes in the anharmonic approximation shifts their frequencies in the same direction by the same quantity. But 2D computations demonstrate that the forms of 2D potential surfaces are very different, and actually the anharmonic interaction of two modes can result in different frequency shifts of their vibrations, both in quantity and in direction. Assuming that 1D and 2D computations more accurately account for anharmonicity of the modes ν_{OH}, $\delta_{\mathrm{OH}}^{\mathrm{ip}}$, $\delta_{\mathrm{OH}}^{\mathrm{oop}}$ themselves and for their anharmonic interaction (while the interaction of these modes with other small-amplitude modes is adequately considered within the scope of the anharmonic approximation), we can combine the advantages of these two approaches. It is thought that the frequencies determined by 1D computations satisfy relation (12). Then, comparing the results of 1D A, 1D B, and 2D AB computations, we can determine the values of χ_{AB} and χ_{BA} on the assumption that

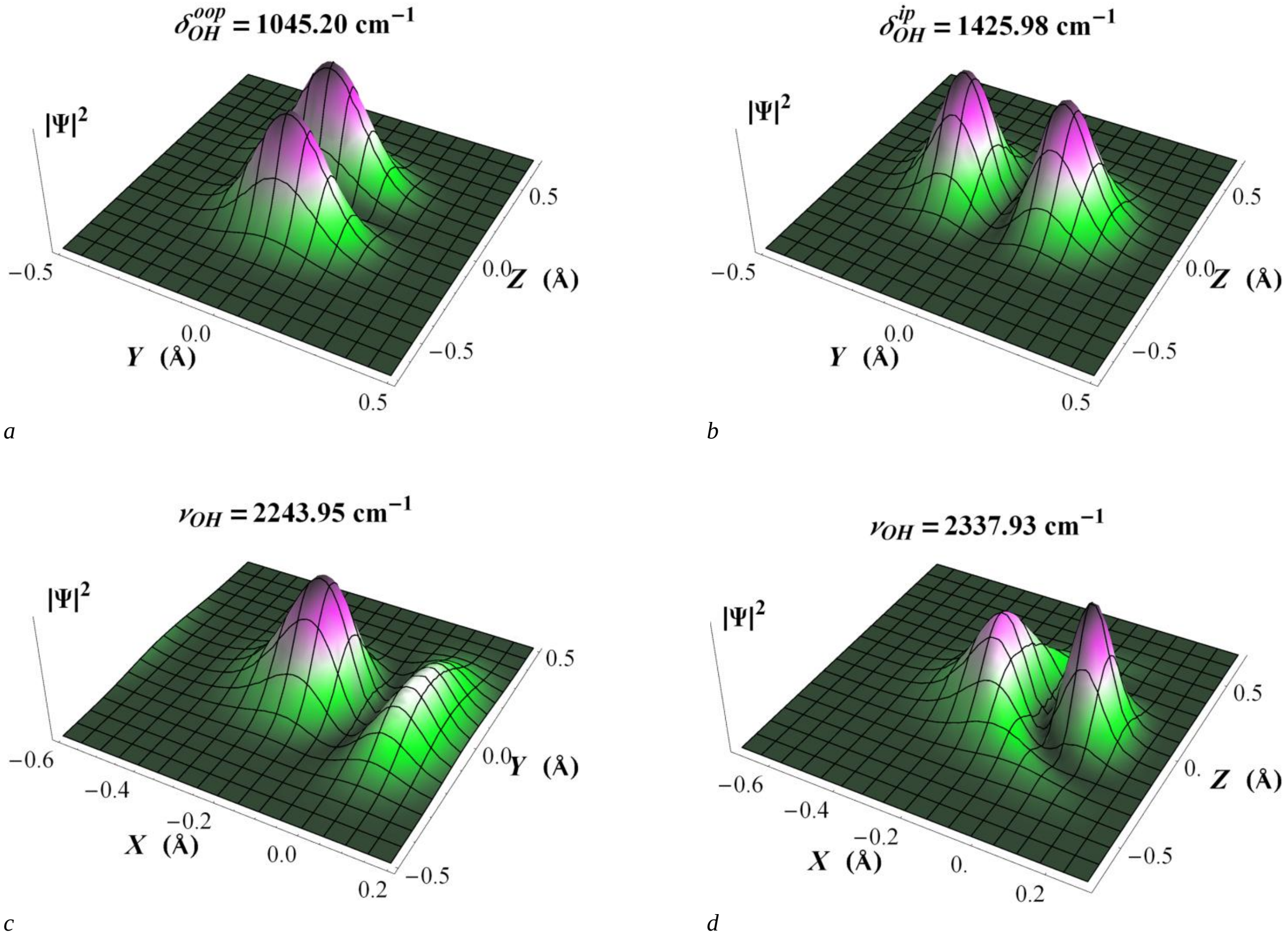

a *b* *c* *d*

Figure 5. Squares of the wave functions for fundamental vibrations of a hydroxyl group.

they may be noncoincident according to the following expression:

$$\frac{1}{2}\chi_{AB} = \nu_A^{2D\,AB} - \nu_A^{1D\,A}. \tag{13}$$

With the use of (13) and of the data $\nu_A^{2D\,AB}$ and $\nu_A^{1D\,A}$ listed in Tables 2 and 4, we can find that $\chi_{6,12} = -50.8$ cm^{-1}; $\chi_{6,23} = 135.4$ cm^{-1}; $\chi_{12,6} = -70.3$ cm^{-1}; $\chi_{12,23} = 19.1$ cm^{-1}; $\chi_{23,6} = -144.9$ cm^{-1}; $\chi_{23,12} = 10.5$ cm^{-1}. Next we find the frequencies of fundamental vibrations using the following expression:

$$\nu_A^{fund} = \nu_A^{1D\,A} + \frac{1}{2}(\chi_{A,B} + \chi_{A,C}) + \frac{1}{2}\sum_{j=1}^{N} \chi_{A,j}\,,\ j \neq A, B, C, \tag{14}$$

where A,B,C - XYZ, YZX, ZXY and $N = 54$. With the use of the anharmonicity matrix elements, it is found that $\frac{1}{2}\sum_j^N \chi_{6,j} = 34.3$ cm^{-1}, $\frac{1}{2}\sum_j^N \chi_{12,j} = -14.5$ cm^{-1}, $\frac{1}{2}\sum_j^N \chi_{23,j} = -50.7$ cm^{-1} ($j \neq 6,12,23$). Then from (14) we can derive the frequencies of fundamental vibrations: $\nu_{OH}^{fund} = 2345.9$ cm^{-1}, $\delta_{OH}^{ip} = 1375.7$ cm^{-1}, $\delta_{OH}^{oop} = 916.5$ cm^{-1}. Table 1 lists the frequencies of fundamental vibrations of a hydroxyl group with regard to Fermi and Darling-Dennison resonances. For the final comparison, it is expedient to cite the resonance-unperturbed frequencies of fundamental vibrations in the anharmonic approximation: $\nu_{OH}^{fund} = 2228.9$ cm^{-1}, $\delta_{OH}^{ip} = 1418.4$ cm^{-1}, $\delta_{OH}^{oop} = 959.2$ cm^{-1}. Note that the difference in frequencies of bending vibrations in part may be associated with mixing of these modes with other normal modes. This aspect is included in computations realized in the anharmonic approximation, whereas in 1D and 2D computations the harmonic mode interaction is not taken into account. But the differences in frequencies for stretching vibrations of $O-H$ group (2228.9 and 2345.9 cm^{-1}) may be due to the selected approach to representation of the potential energy. As the accuracy of its presentation is much higher in the case of 1D and 2D approaches, it is assumed that in the anharmonic approximation a value of the frequency ν_{OH}^{fund} is underestimated by more than 100 cm^{-1}. The final estimation of the possibilities offered by different approaches must be given by the experiment. As demonstrated by our recent studies forming the basis for a new publication, in the anharmonic approximation ν_{OH}^{fund} for the complex under study in acetonitrile comes to 354.1 cm^{-1}, whereas in 1D approach the frequency of this vibration is equal to 1071.3 cm^{-1}. In an IR absorption spectrum of the complex in acetonitrile a maximum of a wide high-intensity band is found at the frequency $1025\ \mathrm{cm}^{-1}$. This makes it possible to assume that the results obtained using 1D and 2D approaches are quite adequate, being even better for overtones and combined frequencies of these vibrations.

7. Conclusions

The frequencies of stretching and bending vibrations of a hydroxyl group in PyO · TCA complex were computed in the harmonic and anharmonic approximations as well as with the help of 1D and 2D computations for the potential surfaces associated with the motion of a hydroxyl hydrogen atom. In the latter case the vibration frequencies of O – H bond were determined by a numerical solution of the Schrödinger equation, using two different numerical methods for 1D approaches. An intricate form of the potential curves and surfaces necessitates the use of higher degree polynomials for their adequate approximation. The potential surface formed in the plane XOZ is especially intricate. There are several directions along which the energy is growing slowly, leading to an increase in the amplitude of vibrations and to the force interaction of stretching and out-of-plane bending vibrations of a hydroxyl group. Owing to combination of the advantages offered by the anharmonic approximation and 1D or 2D approaches, all the vibrational degrees of freedom and the potential surfaces of a more complex form associated with the motion of a hydroxyl hydrogen atom have been included.

Acknowledgements

The study was partially funded from the European Communitys social foundation under Grant Agreement No. VP1-3.1-ŠMM-08-K-01-004/KS-120000-1756. We thank Prof. Dušan Hadži and Prof. Janez Mavri for many ideas and valuable discussions. This work was performed using computational facilities of joint computational cluster of SSI ``Institute for Single Crystals" and Institute for Scintillation Materials of National Academy of Science of Ukraine incorporated into Ukrainian National Grid.

References

1. S. J. Grabovski (Ed.), Hydrogen Bonding: New Insights, Springer, Dordrecht (2006).
2. D. Hadži (Ed.), Theoretical Treatments of Hydrogen Bonding, John Wiley & Sons Ltd, Chichester (1997).
3. XIX International Conference on Horizons in Hydrogen Bond Research, Göttingen, Germany (2011) http://www.hbond.de.
4. W. A. Herrebout and M. A. Suhm, Phys. Chem. Chem. Phys. 13 (2011) 13858.
5. E. Arunan, G. R. Desiraju, R. A. Klein, J. Sadlej, S. Scheiner, I. Alkorta, D. C. Clary, R. H. Crabtree, J. J. Dannenberg, P. Hobza, H. G. Kjaergaard, A. C. Legon, B. Mennucci, and D. J. Nesbitt, Pure Appl. Chem. 83 (2011) 1619.
6. E. Arunan, G. R. Desiraju, R. A. Klein, J. Sadlej, S. Scheiner, I. Alkorta, D. C., Clary, R. H. Crabtree, J. J. Dannenberg, P. Hobza, H. G. Kjaergaard, A. C. Legon, B. Mennucci, and D. J. Nesbitt, Pure Appl. Chem. 83 (2011) 1637.
7. K. Wendler, J. Thar, S. Zahn, and B. Kirchner, J. Phys. Chem. A 114 (2010) 9529.
8. B. Koeppe, P. M. Tolstoy, and H. H. Limbach, J. Am. Chem. Soc. 133 (2011) 7897.
9. S. J. Ford, O. J. Delamore, J. S. O. Evans, G. J. McIntyre, M. R. Johnson, and Evans I. Radosavljevi I., Chem. Eur. J. 17 (2011) 14942.
10. J. Stare, M. Hartl, L. Daemen, and J. Eckert, Acta Chim. Slov. 58 (2011) 52.
11. C. A. Morrison, M. M. Siddick, P. J. Camp, and C. C. Wilson, J. Am. Chem. Soc. 127 (2005) 4042.
12. G. Pirc, J. Stare, and J. Mavri, J. Chem. Phys. 132 (2010) 224506.
13. G. Pirc, J. Mavri, and J. Stare, Vib. Spectrosc. 58 (2012) 153.
14. I. Matanovi and N. Došli, J. Phys. Chem. A 109 (2005) 4185.
15. N. Došli and O. Kühn, Z. Phys. Chem. 217 (2003) 1507.
16. E. Ochiai, Aromatic Amine Oxides Elsevier, Amsterdam (1967).
17. M. Szafran, J. Mol. Struct. 381 (1996) 39.
18. V. Balevicius, K. Aidas, I. Svoboda, and H. Fuess, J. Phys. Chem. A 116 (2012) 8753.
19. V. Balevicius, Z. Gdaniec, and K. Aidas, Phys. Chem. Chem. Phys. 11 (2009) 8592.
20. E. M. Myshakin, K. D. Jordan, E. L. Sibert III, and M. A. Johnson, J. Chem. Phys. 119 (2003) 10138.
21. W. H. Robertson, E. A. Price, J. M. Weber, J. W. Shin, G. H. Weddle, and M. A. Johnson, J. Phys. Chem. A 107 (2003) 6527.
22. J. Antony, G. von Helden, G. Meijer, and B. Schmidt, J. Chem. Phys. 123 (2005) 014305.
23. M. V. Vener, O. Kuhn, and J. M. Bowman, Chem. Phys. Lett. 349 (2001) 562.
24. D. T. Moore, J. Oomens, L. van der Meer, G. von Helden, G. Meijer, J. Valle, A. G. Marshall, and J. R. Eyler, ChemPhysChem 5 (2004) 740.
25. M. J. Frisch, G. W. Trucks, H. B. Schlegel, G. E. Scuseria, M. A. Robb, J. R. Cheeseman, G. Scalmani, V. Barone, B. Mennucci, G. A. Petersson, H. Nakatsuji, M. Caricato, X. Li, H. P. Hratchian, A. F. Izmaylov, J. Bloino, G. Zheng, J. L. Sonnenberg, M. Hada, M. Ehara, K. Toyota, R. Fukuda, J. Hasegawa, M. Ishida, T. Nakajima, Y. Honda, O. Kitao, H. Nakai, T. Vreven, J. A. J. Montgomery, J. E. Peralta, F. Ogliaro, M. Bearpark, J. J. Heyd, E. Brothers, K. N. Kudin, V. N. Staroverov, R. Kobayashi, J. Normand, K. Raghavachari, A. Rendell, J. C. Burant, S. S. Iyengar, J. Tomasi, M. Cossi, N. Rega, N. J. Millam, M. Klene, J. E. Knox, J. B. Cross, V. Bakken, C. Adamo, J. Jaramillo, R. Gomperts, R. E. Stratmann, O. Yazyev, A. J. Austin, R. Cammi, C. Pomelli, J. W. Ochterski, R. L. Martin, K. Morokuma, V. G. Zakrzewski, G. A. Voth, P. Salvador, J. J. Dannenberg, S. Dapprich, A. D. Daniels, C. Farkas, J. B. Foresman, J. V. Ortiz, J. Cioslowski, and D. J. Fox, Gaussian 09, Revision A.1 (2009).
26. A. D. Becke, J. Chem. Phys. 98 (1993) 5648.
27. C. Lee, W. Yang, and R. G. Parr, Phys. Rev. B. 37 (1988) 785.
28. P. J. Stephens, F. J. Devlin, C. F. Chabalowski, and M. J. Frisch, J. Phys. Chem. 98 (1994) 11623.
29. T. H. Dunning, J. Chem. Phys. 90 (1989) 1007.
30. G. A. Pitsevich, M. Shundalau, M. A. Ksenofontov, and D. S. Umreiko, Global J. Anal. Chem. 2 (2011) 114.
31. G. A. Pitsevich and M. Shundalau, J. Spectrosc. Dyn. 2 (2012) 15.
32. G. Herzberg, Molecular Spectra and Molecular Structure: II. Infrared and Raman Spectra of Polyatomic Molecules, Van Nostrand, Princeton (1945).
33. F. Graf, R. Meyer, T. K. Ha, and R. R. Emst, J. Chem. Phys. 75 (1981) 2914.
34. S. A. Barton and W. R. Thorson, J. Chem. Phys. 71 (1979) 4263.
35. A. Agresti, M. Bacci, and A. Ranfagni, Chem. Phys. Lett. 79 (1981) 100.
36. Mathematica, Wolfram Research, Inc., http://www.wolfram.com/mathematica.

37. V. V. Malyshchyts, L. F. Makarenko, G. A. Pitsevich, and A. A. Sokolsky, In: Abstracts of International Science Conference "Informatization of Education" (2010) p. 327 (in Russian).
38. G. A. Pitsevich and A. E. Malevich, OPJ 2 (2012) 332.

G. A. Pitsevich *et al.*: **Vibrational analysis of hydroxyl group in the pyridine n-oxide/trichloroacetic acid complex using the anharmanic approximation and computations of 1D and 2D potential surfaces.** *J. Spectrosc. Dyn.* 2013, **3:** 19